

ERK activation causes epilepsy by stimulating NMDA receptor activity

Abdolrahman S Nateri^{1,2}, Gennadij Raivich³, Christine Gebhardt⁴, Clive Da Costa¹, Heike Naumann⁵, Martin Vreugdenhil⁶, Milan Makwana³, Sebastian Brandner⁵, Ralf H Adams⁷, John GR Jefferys⁶, Oliver Kann⁴ and Axel Behrens^{1,*}

¹Mammalian Genetics Laboratory, Cancer Research UK, London Research Institute, Lincoln's Inn Fields Laboratories, London, UK, ²Division of Pre-Clinical Oncology, Digestive Diseases Centre, Queen's Medical Centre, School of the Medical and Surgical Sciences, University of Nottingham, Nottingham, UK, ³Perinatal Brain Repair Group, Departments of Anatomy & Obstetrics and Gynaecology, University College London, London, UK, ⁴Institute for Neurophysiology, Charité—Universitätsmedizin Berlin, Berlin, Germany, ⁵Division of Neuropathology, Department of Neurodegenerative Disease, Institute of Neurology, London, UK, ⁶Division of Neuroscience, Department of Neurophysiology, Medical School, University of Birmingham, Edgbaston, UK and ⁷Vascular Development Laboratory, Cancer Research UK, London Research Institute, Lincoln's Inn Fields Laboratories, London, UK

The ERK MAPK signalling pathway is a highly conserved kinase cascade linking transmembrane receptors to downstream effector mechanisms. To investigate the function of ERK in neurons, a constitutively active form of MEK1 (caMEK1) was conditionally expressed in the murine brain, which resulted in ERK activation and caused spontaneous epileptic seizures. ERK activation stimulated phosphorylation of eukaryotic translation initiation factor 4E (eIF4E) and augmented NMDA receptor 2B (NR2B) protein levels. Pharmacological inhibition of NR2B function impaired synaptic facilitation in area cornu ammonicus region 3 (CA3) in acute hippocampal slices derived from caMEK1-expressing mice and abrogated epilepsy *in vivo*. In addition, expression of caMEK1 caused phosphorylation of the transcription factor, cAMP response element-binding protein (CREB) and increased transcription of *ephrinB2*. EphrinB2 overexpression resulted in increased NR2B tyrosine phosphorylation, which was essential for caMEK1-induced epilepsy *in vivo*, since conditional inactivation of *ephrinB2* greatly reduced seizure frequency in caMEK1 transgenic mice. Therefore, our study identifies a mechanism of epileptogenesis that links MAP kinase to Eph/Ephrin and NMDA receptor signalling.
The EMBO Journal (2007) 26, 4891–4901. doi:10.1038/sj.emboj.7601911; Published online 1 November 2007
Subject Categories: neuroscience; molecular biology of disease

*Corresponding author. Mammalian Genetics Laboratory, Cancer Research UK, London Research Institute, Lincoln's Inn Fields Laboratories, 44, Lincoln's Inn Fields, London WC2A 3PX, UK. Tel.: +44 207 269 3361; Fax: +44 207 269 3581; E-mail: axel.behrens@cancer.org.uk

Received: 10 August 2007; accepted: 10 October 2007; published online: 1 November 2007

Keywords: cre/loxP; ephrins; epilepsy; ERK; MEK1; NMDA receptor

Introduction

Epilepsies comprise a remarkably diverse collection of disorders that have an effect on millions of people worldwide (Logroscino *et al*, 2005). Current therapy is symptomatic and many suffer from seizures that cannot be readily controlled by current antiepileptic medications. Neither an effective prophylaxis nor a cure for any of these disorders is available except for neurosurgical resection of epileptic tissue in selected instances. It remains unclear how pathological levels of neuronal activity in the form of focal seizures might be triggered by the cellular and molecular mechanisms underlying epileptogenesis.

Extracellular signal-regulated kinases 1 and 2 (ERK1 and ERK2) are essential components of pathways through which signals received at membrane receptors are converted into specific changes in protein function and gene expression (Chen *et al*, 2001; Pearson *et al*, 2001). As with other members of the mitogen-activated protein (MAP) kinase family, ERK1 and ERK2 are activated by phosphorylations catalysed by dual-specificity protein kinases known as MAP/ERK kinases (MEKs). ERK kinases are the only known substrates of MEK1 and MEK2 (Chen *et al*, 2001).

Extracellular stimuli such as neurotransmitters, neurotrophins and growth factors in the brain regulate critical cellular events, including synaptic transmission, neuronal plasticity, morphological differentiation and survival. The ERK kinases are abundantly expressed in the central nervous system and are activated in response to various physiological stimuli associated with synaptic activity and plasticity, most notably calcium influx and neurotrophins, but also during pathological events such as brain ischaemia and epilepsy (Pearson *et al*, 2001; Otani *et al*, 2003; Merlo *et al*, 2004; Sweatt, 2004; Thomas and Haganir, 2004). The substrates of the ERK pathway include numerous proteins with a diverse set of functions, with protein kinases forming a particularly important subset of ERK1/2 targets. ERK can activate several classes of kinases, including the ribosomal S6 kinase (RSK) and MAPK-interacting kinase (Mnk) protein families (Chen *et al*, 2001). Thus MEK/ERK signalling controls biological processes either by directly phosphorylating substrates or indirectly by changing the activity of other kinases.

ERK signalling plays an important role in transcriptional regulation by phosphorylating and thereby modulating the activity of transcription factors (Treisman, 1996). ERK can also alter transcription indirectly, for example through activation of RSKs which phosphorylate, among other substrates, the cAMP response element-binding protein (CREB) at serine 133 (Weeber and Sweatt, 2002). Moreover, ERK also

positively regulates translational efficiency by controlling the phosphorylation of translational initiation factors (Herbert *et al*, 2002; Ueda *et al*, 2004). Recent evidence has shown that neuronal activity-dependent modulation of translation initiation factor activity by the ERK MAPK signalling pathway plays an important role in long-lasting forms of synaptic plasticity and memory (Kelleher *et al*, 2004).

To investigate the consequences of ERK activation in neurons, we employed conditional brain-specific expression of a caMEK1 to show that ERK activation causes spontaneous epileptic seizures. Mechanistically, our study identifies NMDA receptor 2B (NR2B) as a novel target for both translational and for transcriptional regulation by ERK.

Results

Transgenic brain-specific MEK1 overexpression causes epilepsy

Although ERK signalling is implicated in many biological processes, how and why activation of the MEK/ERK pathways results in distinct biological outputs is unclear. Loss-of-function studies in the mouse have yielded important clues about ERK function (Mazzucchelli *et al*, 2002; Fischer *et al*, 2005), but the interpretation of the mutant phenotypes has been complicated by genetic redundancy as the ERK kinases ERK1 and ERK2 are encoded by two different genes (Chang and Karin, 2001; Chen *et al*, 2001). Because of this redundancy, it is possible that essential roles of MAP kinase signalling have remained undetected. Therefore, we devised a strategy that allows to reproducibly activate ERK kinase signalling in mice.

To investigate the significance of ERK activation in the brain, we generated transgenic mice allowing the overexpression of a constitutively active form of the ERK kinase MEK1 (MEK1-LA; Robinson *et al*, 1998). A cassette encoding a fusion protein of β -galactosidase and NeoR (β geo) flanked by loxP sites prevents the expression of constitutively active MEK1 before cre-mediated recombination (β geo-caMEK1) (Figure 1A). Floxed single transgenic mice were crossed with Nestin-cre transgenic mice previously shown to provide ubiquitous brain-specific cre activity (Tronche *et al*, 1999; Raivich *et al*, 2004). Southern blot analysis confirmed efficient removal of the floxed β geo selection cassette in the brain (Figure 1B). In the absence of Cre recombinase, endogenous MEK1 protein was readily detectable in the brains of β geo-caMEK1 single transgenic mice (Figure 1C). caMEK1 transgene expression was induced in β geo-caMEK1;Nestin-cre+ double transgenic mice (designated caMEK1^{AN} mice), to protein levels comparable to endogenous MEK1. Whereas total ERK protein levels were unaltered in caMEK1^{AN} mice, a 2- to 3-fold increase in phosphorylated ERK (P-ERK) was detectable in total brain extracts (Figure 1C). caMEK1^{AN} mice developed normally and were indistinguishable from control littermates until early adulthood. Rotarod tests revealed normal motor function in 5-week-old caMEK1^{AN} mice (Figure 1D). However, starting from 6–8 weeks of age, all caMEK1^{AN} mice exhibited spontaneous epileptic seizures, which were often associated with behavioural arrest and forelimb myoclonus (Supplementary movie 1). These seizures occurred throughout the lifetime of caMEK1^{AN} mice, although seizures appeared less frequently in older (8–14 months) mice (data not shown). *In vivo*

electrophysiological recording from microwire electrodes positioned in the hippocampus revealed electrographic seizures in caMEK1^{AN} mice (Figure 1E). Quantification of seizure frequencies showed that caMEK1^{AN} mice had frequent phenotypical seizures (on average 6.2 seizures per mouse within a 7 h observation time), whereas wild-type mice were seizure-free (Figure 1F).

caMEK1^{AN} mice had normal brain histology and normal expression of neural markers such as NeuN, MAP-2, neurofilament, parvalbumin and synaptophysin (Figure 2A–H; and data not shown). Visualization of mossy fibre arborization with Timm's stain did not reveal differences between caMEK1^{AN} and control mice, arguing against aberrant mossy fibre sprouting as a cause of epilepsy (Figure 2I and J). However, caMEK1^{AN} mice showed a reactive gliosis, an activation of astrocytes characterized by increased GFAP expression, which is commonly seen in response to epileptic seizures (Heinemann *et al*, 1999) (Figure 2K–N). Surprisingly, despite the occurrence of frequent seizures, caMEK1^{AN} mice could survive for over 1 year (which is the longest time period they were kept). The hippocampi of 13-month-old caMEK1^{AN} mice did not show signs of neuronal demise as judged by absence of cells staining for FluoroJade and TUNEL and showed no signs of hippocampal sclerosis (Supplementary Figure 1 and data not shown). Thus, ERK activation triggers epilepsy without causing widespread neuronal death.

Although histological analysis suggested that neuronal organization was normal in caMEK1^{AN} mice, we were unable to rule out that caMEK1 overexpression caused subtle developmental defects. To exclude more directly that the observed epilepsy was due to impaired neuronal development, the β geo-caMEK1 mice were crossed with CamKII-cre transgenics, which directs preferential excision of floxed sequences in the postnatal forebrain (caMEK1^{Afb} mice), with recombination becoming detectable 2–3 weeks after birth (Minichiello *et al*, 1999). caMEK1^{Afb} mice displayed a similar phenotype as caMEK1^{AN} mice since they also were showing spontaneous seizures (data not shown and Figure 6A). This strengthens the notion that the epileptic seizures caused by caMEK1 overexpression are not a consequence of a defect of neuronal development.

Increased levels of P-ERK in caMEK1^{AN} mice

The CamKII-cre transgene expression is confined to the cortex, striatum and hippocampus, with little cre activity detectable elsewhere in the brain (Minichiello *et al*, 1999; Fan *et al*, 2001), implicating these brain regions in caMEK1-induced epilepsy. Immunohistochemical (IHC) detection of P-ERK revealed higher levels of P-ERK throughout the brain in caMEK1^{AN} compared to β geo-caMEK1 or wild-type non-transgenic littermates (Figure 3A–F). P-ERK was localized to different cellular compartments in different neuronal cell types, as noted previously (Thomas and Huganir, 2004). Remarkably, the highest P-ERK staining in the hippocampus was detected in the stratum lucidum, the region located between the dentate gyrus and the cornu ammonicum region 3 (CA3) where the mossy fibre synapses are localized (Figure 3C and D arrowheads). A similar, but weaker, P-ERK staining was observed in the stratum lucidum of control mice, in agreement with previous reports (Sananbenesi *et al*, 2002). Moreover, P-ERK was also increased in the soma of pyramidal

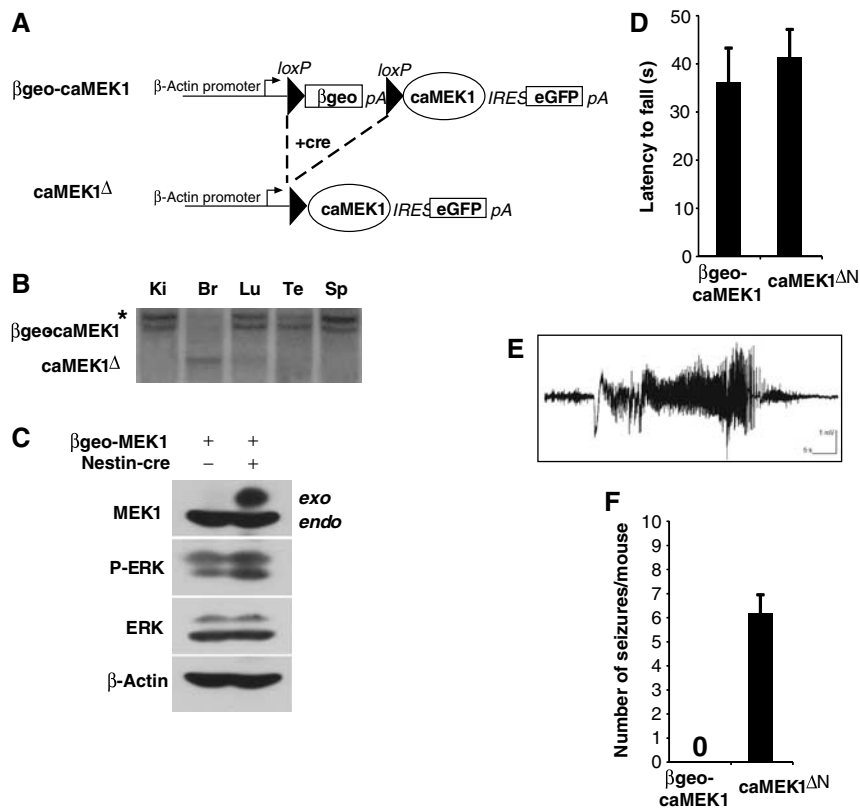


Figure 1 Generation and characterization of mice expressing caMEK1 in the brain. (A) Scheme of the β geo-caMEK1 construct before and after Cre recombination. When these single transgenic mice are crossed with *Cre* transgenic mice, the β geo cassette is excised and the caMEK1 cDNA is expressed. (B) Southern blot analysis of various tissues of caMEK1 Δ mice. Ki, kidney; Br, brain; Lu, lung; Te, testes; Sp, spleen. *Indicates partially digested, unspecific band. (C) Protein lysates from unrecombined β geo-caMEK1 and caMEK1 Δ hippocampi were analysed for MEK1, dually phosphorylated ERK (P-ERK), total ERK and β -actin (loading control) expression. (D) Rotarod performance of 5-week-old β geo-caMEK1 and caMEK1 Δ mice ($n = 6$ for each group). Latency time to fall off an accelerating rotarod is indicated \pm s.e.m. (E) Electrographic seizure recorded from the hippocampus of a caMEK1 Δ mouse during a behavioural seizure dominated by forelimb myoclonus using *in vivo* electrophysiological recording with a radiotelemetry system from microwire electrodes positioned in the hippocampus. (F) Quantification of epileptic seizures in caMEK1 Δ and β geo-caMEK1 mice. Seven mice per genotype were analysed for 7 h, data are presented \pm s.e.m.

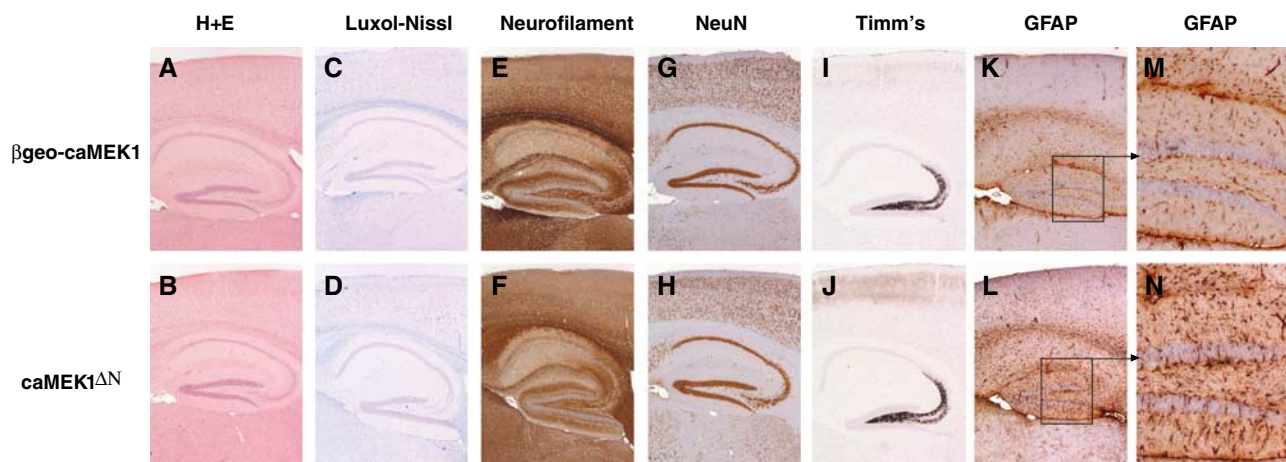


Figure 2 caMEK1 overexpression does not interfere with neuronal development. Haematoxylin and eosin (H + E) staining (A, B), Luxol-Nissl staining (C, D), immunohistochemistry (IHC) for neurofilament (E, F), neuronal nuclei (NeuN; G, H), Timm's stain (I, J) and IHC for GFAP (K–N), was performed on brain sections from 10-week-old β geo-caMEK1 and caMEK1 Δ mice. Rectangles in K and L are magnified in M and N.

neurons of caMEK1 Δ hippocampi (Figure 3C and D). In cortical neurons, P-ERK was located mostly in the nucleus (Figure 3E, F and F'). Thus, caMEK1 overexpression causes ERK activation in both cortex and hippocampus, but

the location of activated ERK differs between neuronal cell types.

As the *in vivo* electrophysiological recording indicated an important role of the hippocampus for caMEK1-induced

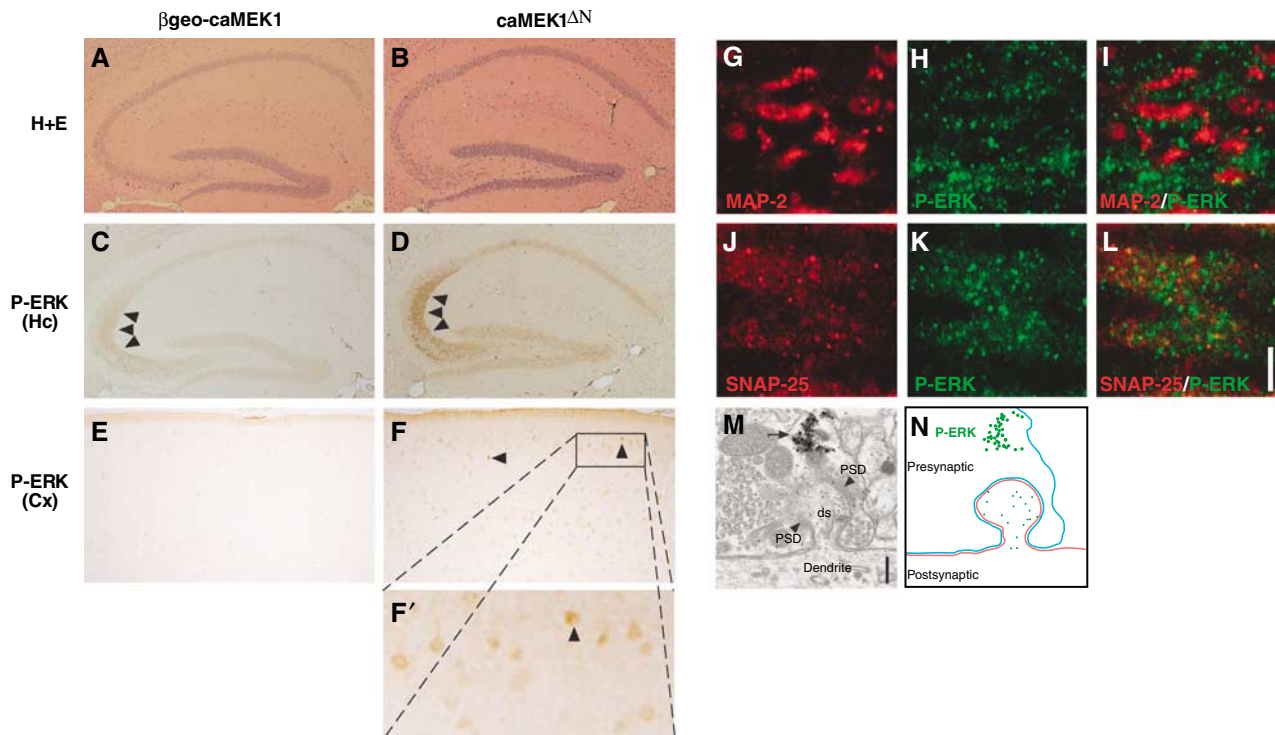


Figure 3 Localization of ERK activation in caMEK1 Δ N mice. (A, B) Histological analysis (haematoxylin and eosin staining (H + E)) of hippocampal sections of β geo-caMEK1 and caMEK1 Δ N mice (8 weeks old). Immunohistochemistry for phosphorylated ERK (P-ERK) on hippocampal (Hc; C, D) and cortical sections (Cx; E, F, F') of β geo-caMEK1 and caMEK1 Δ N mice (8 weeks old). Arrowheads in C, D and F indicate P-ERK staining. Double immunofluorescence for MAP-2 (red; G) and P-ERK (green; H) and the merged image (I); and for SNAP-25 (red; J) and P-ERK (green; K) and the merged image (L) on frozen sections encompassing the stratum lucidum of caMEK1 Δ N mice. Scale bar indicates 5 μ m. (M) EM photographs of P-ERK staining. ds, dendritic spine; PSD, postsynaptic density; arrow indicate P-ERK staining. Scale bar indicates 200 nm. (N) Schematic representation of EM picture shown in (M).

epilepsy, we investigated in more detail the location of P-ERK in the stratum lucidum. Immunofluorescence studies on microdissected stratum lucidum from caMEK1 Δ N hippocampi showed P-ERK staining in the territory marked by the pre-synaptic marker SNAP-25, whereas immunoreactivity for P-ERK and the postsynaptic marker MAP-2 overlapped less well (Figure 3G–L). To further characterize the localization of P-ERK, we employed immunoelectron microscopy. Strong P-ERK staining was found in synaptic terminals of mossy fibres, but postsynaptic staining in dendritic spines was also detectable (Figure 3M and N). Thus, P-ERK is present at both sides of the mossy fibre synapse.

ERK activity regulates NR2B protein expression

To investigate the molecular mechanisms underlying caMEK1-induced epilepsy, we tested whether ERK signalling affected *N*-methyl-D-aspartate receptors (NMDARs). NMDARs are heteromeric complexes containing both NR1 and NR2 subunits located at the postsynaptic side of excitatory synapses and regulate the influx of Ca²⁺ ions (Cull-Candy *et al*, 2001; Prybylowski and Wenthold, 2004). NMDARs have been strongly implicated in epileptogenesis and have been suggested as therapeutic targets for anti-epileptic treatment (Cull-Candy *et al*, 2001; Palmer, 2001). Whereas the mRNA levels of the NMDAR subunits NR2A and NR2B were unchanged in the hippocampi of caMEK1 Δ N mice (Figure 4A), there was a significant increase in NR2B, but not NR1 or NR2A, protein levels (Figure 4B). This suggested that NR2B is

regulated by ERK signalling through a post-transcriptional mechanism.

The eukaryotic translation initiation factor 4E (eIF4E) is a well-characterized substrate of the MEK signalling pathway, and phosphorylation of eIF4E positively regulates translation efficiency. Whereas total eIF4E protein levels were unaltered, eIF4E phosphorylation was augmented in hippocampal protein extracts from caMEK1 Δ N mice (Figure 4C).

To directly investigate whether ERK activity regulates NR2B translation, we used the SHSY5Y neuronal cell line as a model system. SHSY5Y cells have high endogenous ERK activity and substantial eIF4E phosphorylation, which were both greatly reduced by treatment with the pharmacological MEK1 inhibitor U0126 (Figure 4D). To address whether ERK signalling controls NR2B translation, we performed metabolic labelling studies. The experiment was carried out in the presence of Actinomycin-D and proteasome inhibitors, to exclude potential effects of ERK on NR2B transcription or stability. ³⁵S-labelling revealed that in the absence of ERK activity, the amount of *de novo* synthesized NR2B protein was reduced by 50–70% compared to control-treated cells (Figure 4E). Thus, ERK signalling regulates NR2B abundance in neurons *in vivo* and *in vitro*.

Ifenprodil is representative of a class of NMDA receptor antagonists (phenylethanolamines) with high selectivity for NR2B-containing receptors (Kew and Kemp, 1998; Chenard and Menniti, 1999). To test the functional significance of NR2B upregulation, NR2B function was pharmacologically

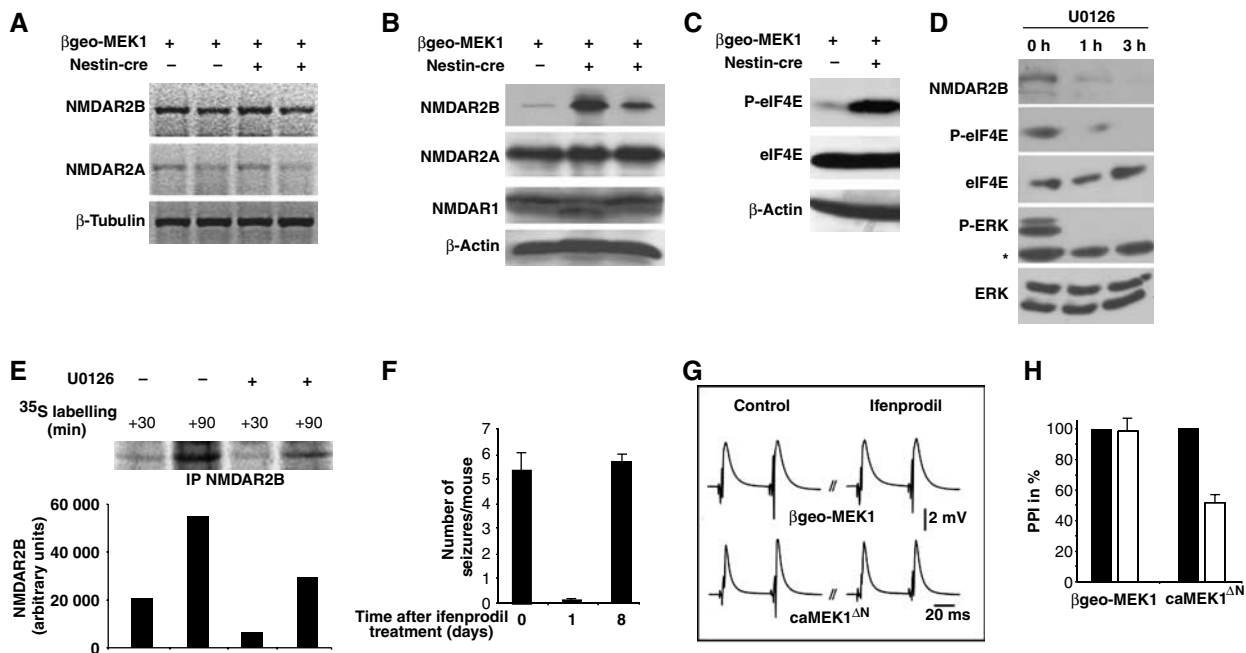


Figure 4 Increased NR2B protein levels in caMEK1^{ΔN} mice. (A) RT-PCR analysis of RNA isolated from unrecombined βgeo-caMEK1 and caMEK1^{ΔN} hippocampi (two independent mice each) for *NMDAR2A*, *NMDAR2B* and β-tubulin (loading control) expression. (B) Western analysis of protein lysates from one unrecombined βgeo-caMEK1 and two independent caMEK1^{ΔN} hippocampi (8 weeks old) for NMDAR1, NMDAR2A, NMDAR2B and β-actin (loading control) expression. (C) Western analysis of protein lysates from unrecombined βgeo-caMEK1 and caMEK1^{ΔN} hippocampi for eIF4E, phosphorylated eIF4E (P-eIF4E) and β-actin (loading control) expression. (D) Western analysis of protein lysates from SHSY5Y cells (untreated or treated for 1 and 3 h with 10 μM U0126) for eIF4E, phosphorylated eIF4E (P-eIF4E), ERK, phosphorylated ERK (P-ERK) and NR2B expression. *Indicates unspecific band. (E) Upper panel: SHSY5Y cells were metabolically labelled with ³⁵S with or without 10 μM U0126. At the indicated time points, NMDAR2B protein was immunoprecipitated (IP), IPs were separated by SDS-PAGE and exposed to X-ray film. Lower panel: Quantification of band intensity using Phosphoimager software. (F) Quantification of epileptic seizures in caMEK1^{ΔN} mice after a single injection of ifenprodil (1 μg/g body weight). Seizures were scored for 7 h in seven ifenprodil-treated caMEK1^{ΔN} mice, either before treatment, or on days 1 and 8 after ifenprodil injection. (G) Ifenprodil reduces the paired-pulse index in hippocampal area CA3a of caMEK1^{ΔN} mutant mice. Traces of extracellular field potential responses as evoked by orthodromic paired-pulse stimulation of area CA3a. Note the smaller population spike amplitude as evoked by the second stimulus in caMEK1^{ΔN} mutant mice in the presence of 10 μM ifenprodil (right lower trace) as compared to control conditions. (H) Histogram illustrating the significant reduction of the paired-pulse index (PPI, normalized to 100% of control) by ifenprodil in slices from caMEK1^{ΔN} mutant mice versus control treatment ($P < 0.01$, $n = 6$) and versus ifenprodil treatment in wild type ($P < 0.05$). The difference in the wild type (control treatment versus ifenprodil) is insignificant ($P = 0.9$, $n = 8$). Error bars indicate s.e.m.

inhibited in caMEK1^{ΔN} mice. Strikingly, a single injection of ifenprodil almost completely abrogated the epileptic seizures caused by overexpression of caMEK1. However, after 8 days the seizure frequency was again comparable to untreated caMEK1^{ΔN} animals (Figure 4F).

To further explore the functional significance of increased NR2B protein levels in the CA3 area directly, we tested the effects of ifenprodil on synaptic transmission in acute hippocampal–entorhinal cortex slices from wild-type and caMEK1^{ΔN} mutant mice. Extracellular field potentials were recorded in CA3 in response to orthodromic electrical stimulation. Paired-pulse stimulation resulted in a more than 3-fold increase in population spike amplitudes of the second field potential response in both wild type and mutant, indicating synaptic facilitation (Figure 4G). Bath application of ifenprodil (10 μM, 60 min) had no effect in controls, but significantly reduced the paired-pulse index (PPI) in caMEK1^{ΔN} mutants (Figure 4H). These data indicate a considerably higher contribution of functional NR2B receptor subunits in synaptic transmission in caMEK1^{ΔN} mutants. Ifenprodil reduced spontaneous excitatory postsynaptic currents in hippocampal CA3 neurons of caMEK1^{ΔN} mutant mice (Supplementary Figure 2). Thus, the effects of ifenprodil on caMEK1^{ΔN} mutants both

in vivo and *in vitro* are in agreement with the notion that increased NR2B function contributes to ERK-induced epilepsy.

Increased transcription of *ephrinB2* in caMEK1^{ΔN} mice

Western blot analysis of caMEK1^{ΔN} hippocampi revealed increased phosphorylation of the transcription factor CREB, a known mediator of ERK signalling (Pearson *et al*, 2001; Weeber and Sweatt, 2002) (Figure 5A). Activated CREB is an important regulator of neuronal function and CREB phosphorylation is strongly induced by a plethora of stimuli, including excitotoxins (Lonze and Ginty, 2002). To determine whether changes in neuronal transcription contributed to epilepsy induced by caMEK1 overexpression, the transcriptome of caMEK1^{ΔN} and control βgeo-caMEK1 hippocampi was compared. Microarray analysis showed not only increased mRNA levels of tyrosine hydroxylase and *C/EBPβ*, known CREB target genes (Kim *et al*, 1993; Niehof *et al*, 1997) but also genes that had previously not been associated with ERK signalling were deregulated (Supplementary Table 1). Most notably, the transcription of *ephrinB2*, a ligand for the Eph family of tyrosine kinases (Klein, 2004), was increased, whereas there was no alteration in the expression of the

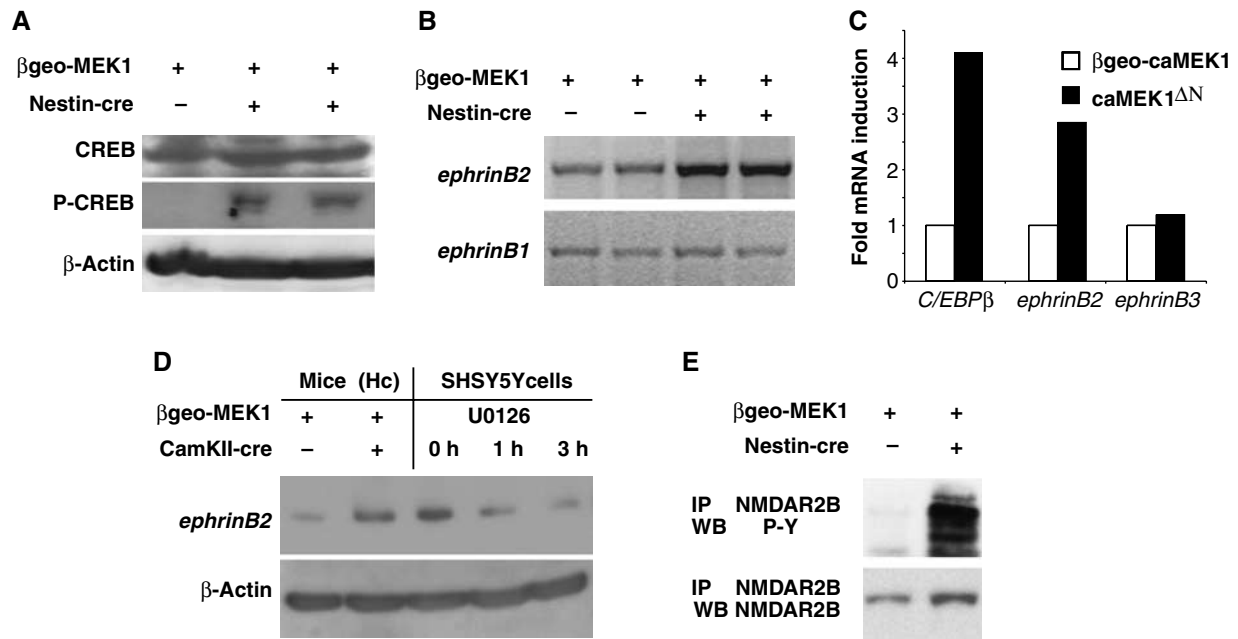


Figure 5 *EphrinB2* transcription is increased in caMEK1^{AN} hippocampi. (A) Protein lysates from unrecombined β geo-caMEK1 and caMEK1^{AN} hippocampi (two independent mice) were analysed for CREB, phosphorylated CREB (P-CREB) and β -actin (loading control) protein expression. (B) RT-PCR analysis of RNA isolated from unrecombined β geo-caMEK1 and caMEK1^{AN} hippocampi (two independent mice each) for *ephrinB1* and *ephrinB2* expression. (C) Quantitative RT-PCR analysis of RNA isolated from unrecombined β geo-caMEK1 and caMEK1^{AN} hippocampi for *ephrinB2*, *ephrinB3* and *c/EBPbeta* expression. (D) Western analysis of protein lysates from unrecombined β geo-caMEK1 and caMEK1^{AN} hippocampi, or from SHSY5Y cells (untreated or treated for 1 and 3 h with 10 μ M U0126) for *ephrinB2* and β -actin (loading control) expression. (E) NMDAR2B protein was immunoprecipitated (IP), IPs were separated by SDS-PAGE and western blot analysis for NMDAR2B and phosphorylated tyrosine was performed. Ten-week old mice were used for both mRNA and protein isolation.

homologous *ephrinB1* (Figure 5B). Quantitative PCR analysis confirmed increased expression of *C/EBP β* and *ephrinB2*, but revealed no differences in *ephrinB3* transcription (Figure 5C). Also, *ephrinB2* protein levels were increased in caMEK1^{AN} hippocampi and pharmacological MEK inhibition reduced *ephrinB2* protein levels in SHSY5Y cells (Figure 5D). CREB has recently been shown to bind the *ephrinB2* promoter in a genome-wide approach to characterize CREB target genes, suggesting that *ephrinB2* may be a direct target of CREB (Zhang *et al*, 2005). We were especially interested in *ephrinB2* as a target for ERK signalling because previous work had linked *ephrinB2* function to NMDA receptor signalling at synapses. Trans-synaptic interactions between post-synaptic EphB receptors and presynaptic B-ephrins are necessary for the induction of mossy fibre long-term potentiation (LTP) (Contractor *et al*, 2002). Treatment of cultured neurons with *ephrinB2* led to tyrosine phosphorylation specifically of the NR2B subunit (Takasu *et al*, 2002). We therefore investigated whether the phosphorylation status of NR2B was altered in caMEK1-overexpressing mice. NR2B tyrosine phosphorylation was greatly augmented in caMEK1^{AN} mutant mice (Figure 5E), suggesting that stimulation of NR2B phosphorylation, in addition to increasing NR2B protein levels, is a second mechanism by which ERK signalling augments NR2B activity.

***EphrinB2* is required for NR2B phosphorylation and epilepsy in caMEK1^{AN} mice**

To directly test the relevance of *EphrinB2* as a target of ERK signalling, we crossed mice harbouring a floxed allele of

ephrinB2 (*ephrinB2*^{fl}) (Grunwald *et al*, 2004) to caMEK1^{AN} mice. Spontaneous seizures were significantly reduced in β geo-caMEK1; *ephrinB2*^{fl/fl}; CamKII-cre + compound mutant mice (caMEK1^{AN}; *ephrinB2*^{AN} mice). Quantification revealed that the absence of *ephrinB2* reduced the frequencies of seizures by 80% (Figure 6A). Probably as a consequence, astrocytic gliosis was not observed in caMEK1^{AN}; *ephrinB2*^{AN} mice (Figure 6B). Hippocampal NR2B protein levels were increased to similar extents in mice overexpressing caMEK1 and in caMEK1^{AN}; *ephrinB2*^{AN} double mutants, suggesting that *EphrinB2* is not involved in the regulation of NR2B translation by caMEK1 (Figure 6C). In contrast, inactivation of *ephrinB2* significantly reduced tyrosine phosphorylation of NR2B seen in caMEK1^{AN} mutant mice, to levels detectable in control mice (Figure 6C). Tyrosine residue 1472 (Tyr-1472) within NR2B is a major phosphorylation site for Src-family kinases (Nakazawa *et al*, 2001; Takasu *et al*, 2002). caMEK1 overexpression increased Tyr-1472 phosphorylation compared to controls; however, in caMEK1^{AN}; *ephrinB2*^{AN} double mutants Tyr-1472 phosphorylation was significantly reduced (Figure 6D). *EphrinB2* is thus essential for NR2B phosphorylation and epileptogenesis triggered by caMEK1 *in vivo*.

Discussion

We have generated a mouse model that allows for the activation of ERK signalling *in vivo* by conditional cre/loxP-mediated overexpression of caMEK1. A main advantage of this approach is its great versatility, since by choosing the appropriate cre-expressing transgenic lines, any tissue or

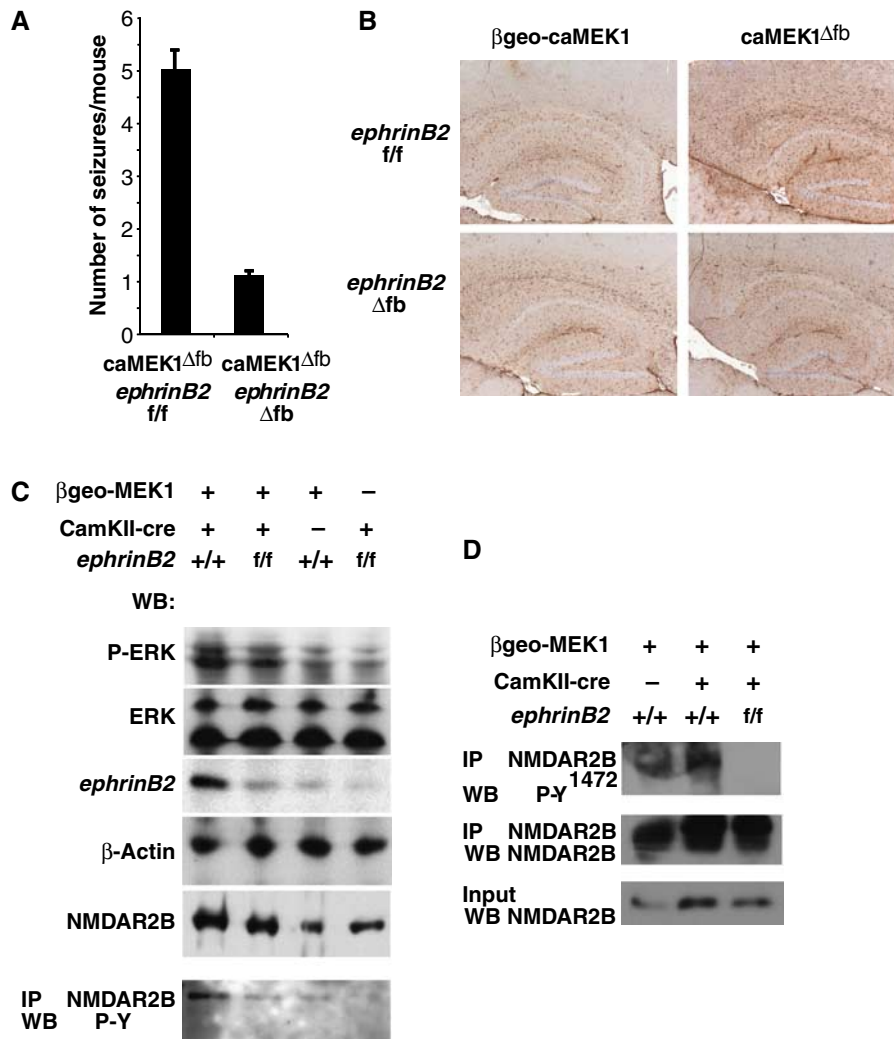


Figure 6 EphrinB2 is required for caMEK1-induced NMDAR2B tyrosine phosphorylation and epilepsy. (A) Quantification of epileptic seizures in 8-week old caMEK1^{Δfb} and caMEK1^{Δfb}; ephrinB2^{Δfb} double mutant mice. Five mice per genotype were analysed for 7 h. Error bars indicate s.e.m. (B) Immunohistochemistry for GFAP was performed on brain sections from unrecombined βgeo-caMEK1 and caMEK1^{Δfb} hippocampi, either wild-type for or lacking EphrinB2. (C) Western analysis of protein lysates from unrecombined βgeo-caMEK1 and caMEK1^{Δfb} hippocampi, either wild-type for or lacking EphrinB2, for ERK, phosphorylated ERK (P-ERK), ephrinB2, NMDAR2B and β-actin (loading control) expression. Lowest panel: NMDAR2B protein was immunoprecipitated (IP), IPs were separated by SDS-PAGE and western blot analysis for phosphorylated tyrosine was performed. (D) NMDAR2B protein was immunoprecipitated (IP) from protein lysates from unrecombined βgeo-caMEK1 and caMEK1^{Δfb} hippocampi, either wild-type for or lacking EphrinB2, IPs were separated by SDS-PAGE and western blot analysis for total NMDAR2B protein and NMDAR2B phosphorylated at tyrosine 1472 (P-Y1472) was performed. In A–D, 8–10-week-old mice were used.

biological process can be studied. In this study, we describe that brain-specific overexpression of caMEK1 in mice causes spontaneous epileptic seizures.

Localization of phosphorylated ERK

caMEK1^Δ mice showed robust activation of ERK signalling and phosphorylation of downstream pathway components. IHC revealed that P-ERK staining in the hippocampus was most pronounced in the stratum lucidum. This localization is in contrast to the predominantly nuclear localization of active ERK that is commonly seen in many cell types and that we also observed in cortical neurons (Ranganathan *et al*, 2006). It is noteworthy that the location of activated ERK is not unique: the neurotrophin receptor TrkB is ubiquitously expressed throughout the brain, but during epileptogenesis TrkB undergoes phosphorylation at the mossy fibre synapse

and active phosphorylated TrkB receptor is specifically detected in the stratum lucidum (Binder *et al*, 1999; He *et al*, 2002). Conditional neuron-specific deletion of TrkB prevented epilepsies in the kindling model, underscoring the functional relevance of TrkB activation (He *et al*, 2004). The concomitant activation of both TrkB and ERK in the same anatomical region indicates that the stratum lucidum is a particularly important location for pro-epileptogenic signalling events.

Regulation of NR2B translation by ERK

Activation of ERK signalling increased NR2B protein levels in protein extracts from caMEK1^Δ hippocampi. Importantly, modulation of ERK signalling also affected NR2B protein expression in neuronal cell lines (Figure 4D), suggesting that deregulation of NR2B is a direct consequence of changes in ERK activity (Figure 7). However, it should be noted that

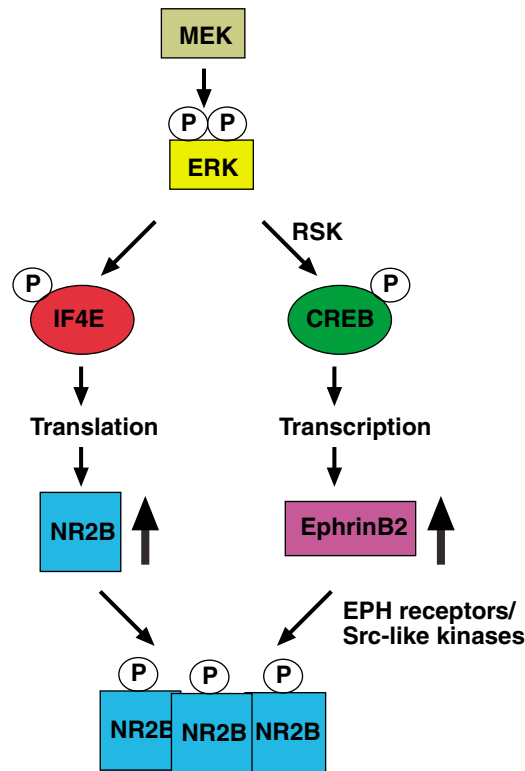


Figure 7 Model of regulation of NR2B function by ERK signalling. Schematic representation of the molecular pathways directing transcriptional and translational regulation of NR2B function by MEK1/ERK signalling.

while our data are consistent with the notion that NR2B is one of the translational targets of ERK signalling, we cannot formally exclude that ERK signalling also affects other aspects of NR2B biology, such as receptor internalization and recycling. It is noteworthy that the increase in NR2B tyrosine phosphorylation cannot account for increased NR2B levels since *caMEK1^{Δfb}*; *ephrinB2^{Δfb}* double mutants show wild-type levels of NR2B tyrosine phosphorylation but still increased NR2B protein (Figure 6C).

The entorhinal cortex via the perforant path produces most of the input into dentate gyrus (DG) granule cells and onwards to CA3. P-ERK is most highly expressed in DG neurons, and more NR2B in DG neurons could increase the perforant path/DG drive to CA3. In line with this model, targeted deletion of NR1 has recently been shown to decrease firing rates in CA3 neurons (McHugh *et al*, 2007) and NMDA receptors in the dentate gyrus neurons are important for kindling-induced epilepsies (Mody and Heinemann, 1987). In addition, the increased perforant path/DG drive may be further amplified by increases in CA3 NR2B. Thus, we speculate that increased NR2B protein may function both in dentate gyrus granule cells and in CA3 neurons to increase the drive and firing rates of the hippocampal circuit (Figure 7).

The attenuation of epilepsies in ageing *caMEK1^{ΔN}* mice might be due to changes in NMDA receptor function with age. Ageing animals exhibit a decline in NMDA receptor-binding densities and NMDA-stimulated release of transmitters is decreased with age (Gonzales *et al*, 1991). An age-related reduction in binding of glutamate to NMDA-binding sites has

been reported in mice, rats, dogs and monkeys (Tamaru *et al*, 1991; Wenk *et al*, 1991). Thus, it is conceivable that an age-related decline in NMDA receptor activity reduces the frequencies of seizures in old *caMEK1^{ΔN}* mice.

While NR2B translational regulation has not been studied, some work has been carried out on NR2A. Mutational analysis of the NR2A 5'-UTR implicated secondary structure as a major translational impediment and an important biological role for the 5'-UTR of NR2A was further suggested by the unusually high level of sequence conservation among species. In contrast, the 5'-UTR of NR1 did not affect translation and is not conserved (Wood *et al*, 1996). The molecular details of ERK-mediated regulation of NR2B translation are certainly worth investigating as they may reveal interesting insights into the control of synaptic plasticity.

Cross-talk between Eph/Ephrin and NMDA receptor signalling

In addition to increased NR2B translation, ectopic activation of ERK signalling also employs transcriptional mechanisms to regulate the ephrin/Eph and NMDA receptor pathways. In wild-type hippocampus, *EphrinB2* mRNA is expressed in the CA1 and DG neurons, but absent from the CA3 region (Henderson *et al*, 2001; Grunwald *et al*, 2004). In contrast, several Eph receptors that are capable of binding EphrinB2 ligand, including EphB1, EphB2 and EphA4, are present in CA3 neurons (Grunwald *et al*, 2004). Therefore, at the mossy fibre synapse EphrinB2 ligand is expressed presynaptically and Eph receptors are expressed postsynaptically (Klein, 2004). Functional analysis indeed confirmed an important function for Ephrins and Eph receptors in trans-synaptic signalling in the induction of mossy fibre LTP as suggested by their complementary expression patterns (Contractor *et al*, 2002).

Thus, presynaptic *ephrinB2* transcription induced by ERK signalling may signal across the mossy fibre synapse to activate postsynaptic Eph receptors. Ligand binding causes Eph receptor clustering and reciprocal phosphorylation on multiple tyrosine residues. The phosphorylated tyrosines recruit downstream signalling proteins containing SH2 domains, including Src family kinases such as Fyn (Klein, 2004; Murai and Pasquale, 2004). Fyn physically associates with both the EphB and NMDA receptors and Fyn phosphorylates NR2B on tyrosines 1252, 1336 and 1472 (Nakazawa *et al*, 2001). Treatment of primary cortical neurons with recombinant ephrinB2 was shown to cause NMDA receptor tyrosine phosphorylation through activation of EphB receptors and subsequent stimulation of Src family kinases. These ephrinB2-dependent events resulted in increased NMDA receptor-dependent influx of calcium and suggested that ephrinB2 stimulation of EphB modulates the functional consequences of NMDA receptor activation (Takasu *et al*, 2002). This molecular mechanism appears to contribute to *caMEK1*-induced epilepsy since genetic inactivation of *ephrinB2* led to a significant decrease in NR2B tyrosine phosphorylation and the number of epileptic seizures. While this result is in agreement with the notion that ephrin/Eph signalling regulates NR2B tyrosine phosphorylation *in vivo* (Figure 7), we cannot rule out that the reduced numbers of seizures contribute to the decrease in NR2B tyrosine phosphorylation. *ephrinB2* has previously been shown to participate in the regulation of plasticity of CA3/CA1 hippocampal synapses;

however, mossy fibre synapses were not investigated in this study (Grunwald *et al*, 2004). We noted that NR2B tyrosine phosphorylation was not only reduced by the absence of ephrinB2 in caMEK1^{Δb} transgenics but that ephrinB2^{Δb} single mutant mice also showed decreased NR2B tyrosine phosphorylation compared to wild-type control mice (Figure 6C and data not shown). Thus, the control of NR2B phosphorylation by EphrinB2 may be a signalling pathway that contributes to the physiological regulation of synaptic plasticity, and whose hyperactivation in caMEK1^Δ mice leads to epilepsy.

Pharmacological treatment of ERK-induced epilepsies

ERK activation appears to be sufficient to trigger epilepsy in mice and it is therefore conceivable that this pathway may also play an important role in the aetiology of some forms of human epilepsy. Our data suggest that ERK triggers a signalling network that culminates in the augmentation of NR2B function. The importance of NMDAR activity downstream of ERK was confirmed by pharmacological inhibition of NR2B with ifenprodil, which efficiently blocked ERK-induced seizures. In addition to NR2B, other components of the signalling network could also be considered as targets for therapeutic intervention. Genetic inactivation of ephrinB2 significantly reduced the frequency of seizures in caMEK1^{Δb} mutant mice, indicating that Eph receptors could be attractive molecular targets for preventing epilepsy. Most obviously, inhibition of ERK signalling may be of potential clinical benefit. Inhibitors of MEK1 have been identified (Sebolt-Leopold and Herrera, 2004) and it will be worthwhile to test whether these reagents have a therapeutic effect for treatment of epilepsies.

Materials and methods

Mice

The βgeo-caMEK1 transgenic construct was electroporated into embryonic stem cells, stable transfectants were selected and mice were generated according to standard protocols (Behrens *et al*, 1999). βgal staining was used to ensure high transgene expression in ES cells and Southern blot analysis was used to confirm single-copy integration (data not shown). Mice harbouring a floxed ephrinB2 allele have been described previously (Grunwald *et al*, 2004).

Quantification of epilepsies and in vivo electro cortical recordings

Phenotypical epileptic seizures were characterized by arrest of motion, tonic/clonic limb movement and loss of posture (see Supplementary movie 1 for an example). Mice were observed and scored by two independent observers for 7 h/day. Ifenprodil (Sigma) was injected intraperitoneally to a final concentration of 1 μg/g body weight. In response to ifenprodil injection, both control and mutant mice appeared drowsy for 5–10 min, after which animal behaviour returned to normal.

Mouse PhysioTel[®] EA-F20 single channel implantable radio-telemetry transmitters (Data Sciences International, Arden Hills, USA) were used to record from area CA3 in the dorsal hippocampus. A 125-μm Teflon[®]-insulated silver wire (Advent, Eynsham, UK) was soldered to the active lead and the connection was insulated with Dow Corning[®] Silicone 734. A bone screw was attached to the ground lead.

Three mice (25–30 g body weight) were given prophylactic peripheral analgesic treatment 15 min before surgery by subcutaneous injection of 0.2 ml 1:50 dilution Rimadyl[®] vet; 50 mg/ml carprofen (Pfizer, USA). Mice were anaesthetized using isoflurane. The skin from between the ears to half way the back was shaved and swabbed with 70% alcohol. The mouse was placed in a stereotaxic

frame fitted with a mouse adapter (Harvard Apparatus, Holliston, USA). Body temperature was monitored with a rectal probe and maintained at 36–37°C. A ~3 cm incision was made between the eyes and the exposed skull was cleaned with 1% H₂O₂. After removal of the skin a burr hole for electrode placement was made at 2.0 mm posterior 2.0 mm right from bregma and two holes for bone screws were made straddling the hole. The transmitter was placed in a subcutaneous pocket in the scruff and fixed with Prolene[®] 4/0 suture. The ground electrode screw (contacting the cortical surface) and anchor were inserted, followed by the silver wire electrode with the tip located 1.6 mm below the cortical surface. Electrode, leads and screws were fixed to the skull with Simplex Rapid dental acrylic (Howmedica, London, UK). The incision was closed with Prolene[®] 5/0 suture. After surgery, mice were given additional pain relief by subcutaneous injection of 0.05 ml Temgesic[®] (0.3 mg/ml buprenorphin, Schering-Plough, USA) and placed in a warmed recovery cage. Recording of biopotentials, using Dataquest[®] ART software (Data Sciences International), started after 10 days by which time the wound was fully recovered and the mice had adapted to carrying the transmitter.

Electrophysiological recordings

Acute hippocampal-entorhinal cortex slices were prepared using standard techniques (Kann *et al*, 2005). In brief, adult genotyped wild-type and caMEK1^{ΔN} mutant littermates were decapitated under deep diethylether anaesthesia and the brain was quickly removed. Horizontal slices (350 μm) were prepared using a vibratome (VT 1000 S; Leica, Bensheim, Germany) in ice-cold preparation solution (in mM; 87 NaCl, 26 NaHCO₃, 25 glucose, 2.5 KCl, 7 MgCl₂, 1.25 NaH₂PO₄, 0.5 CaCl₂, 75 sucrose, pH 7.4) and directly transferred to a custom-built interface chamber (95% O₂, 5% CO₂). Slices were allowed to recover in artificial cerebrospinal fluid (ACSF; 1.5 ml/min, 36 ± 0.5°C) for at least 1 h before being used for experiments. ACSF contained in mM: 129 NaCl, 21 NaHCO₃, 10 glucose, 3 KCl, 1.8 MgSO₄, 1.25 NaH₂PO₄, 1.6 CaCl₂, pH 7.4. Whole-cell recordings were performed under submerged recording conditions, in the absence of extracellular Mg²⁺ and in the presence of bicuculline (5 μM). The internal patch solution contained in mM: 130 Cs-gluconate, 8 CsCl, 10 HEPES, 10 EGTA, 2 NaCl, 2 Mg-ATP, pH 7.3. Preparation solution and ACSF were saturated with 95% O₂ and 5% CO₂. Salts were from Sigma-Aldrich (Taufkirchen, Germany), ifenprodil hemitartrate and bicuculline methochloride were from Tocris (Bristol, UK).

Extracellular field potentials were recorded at 5 kHz digitization (1 kHz low-pass filter) from stratum pyramidale of area CA3a with microelectrodes (5–10 MΩ), which were filled with 154 mM NaCl solution, using a custom-built amplifier and a commercial interface (CED 1401) with 'Spike2' software (both from Cambridge Electronic Design, Cambridge, UK). For paired-pulse experiments, a bipolar tungsten electrode (10–20 μm tip diameter, ~200 μm tip separation) was positioned in the dentate gyrus to activate fibre tracts to area CA3 and paired pulses (100 μs stimulus duration, 50 ms interval) were delivered every 30 s with submaximal stimuli (about 70% of intensity required to evoke population spikes of maximal amplitude).

Whole-cell recordings were made using a Multiclamp 700B (Axon Instruments, Molecular Devices, USA) and standard techniques (Gebhardt and Cull-Candy, 2006). Patch pipettes pulled from thick-walled borosilicate glass had a resistance of 6–8 MΩ when filled with solution. CA3 pyramidal neurons were identified visually. The access resistance was checked during the recording and the experiments were stopped if the access resistance had changed more than 10%. Data were recorded by Clampex 9 with a sampling rate of 10 kHz and filtered at 2 kHz.

For field potential analysis, 'Signal3' software (Cambridge Electronic Design) was used. Ten field potential responses as evoked by paired pulses were averaged and the population spike amplitude was determined as the amplitude from the first positive peak to the maximal negative peak. The PPI was calculated by dividing the determined population spike amplitude of second by the first paired-pulse response.

Whole-cell recordings were analysed with Clampfit 9. Data are given as mean ± s.e.m. and are derived from at least three mouse preparations per group. Statistical significance was determined using Student's *t*-tests.

Motor function

Mice were accustomed to and trained on the rotarod five times per week between the age of 3 and 5 weeks. Then mice were tested for motor function using the accelerating rotarod (4–40 r.p.m.) (UGO Basile, Varese, Italy) once per day on three consecutive days. The time spent on the rotarod was recorded. The value is the average of the three tests \pm s.e.m.

Biochemistry

Mice were killed by cervical dislocation, and the hippocampus region was quickly dissected and frozen in liquid nitrogen. Cell lysates were homogenized in lysis buffer and protease inhibitor. Immunoblots were carried out as previously described (Nateri *et al*, 2004). Antibodies to NR2B, β -actin (Sigma), NR1, NR2A (Synaptic Systems) and NR2B (Chemicon), phosphorylated NR2B-Y1472 (Sigma), phosphorylated CREB (Ser 133), CREB, eIE4E, phospho-eIE4E, p44/42 MAPK, phospho-p44/42 MAPK (thr202/tyr204), MEK1/2 (Cell Signalling), EphrinB2 (R&D Systems), RSK, phospho-RSK, phosphotyrosine (PY99) (Santa Cruz) were used. For immunoprecipitation, hippocampal lysates were incubated with primary NR2B-specific antibody and bound to protein G sepharose beads. Immunoprecipitated proteins were separated by SDS-PAGE. The gels were transferred to PVDF membranes, and the membranes were immunoblotted with various antibodies as indicated.

Metabolic labelling was carried out in SHSY5Y human neuronal cells that were radioactively labelled with 0.2 mCi of 35 S-methionine and 35 S-cysteine/ml in a labelling medium lacking methionine and cysteine (ICN). Actinomycin-D (5 μ g/ml; Sigma) and proteasome inhibitor I (1 μ g/ml; Calbiochem) were added 30 min before the addition of labelling medium to all samples to prevent *de novo* transcription and protein degradation. Also, 10 μ M MEK inhibitor U0126 (Promega) was added 30 min before the labelling period to specific samples. Cell extracts and immunoprecipitation were carried out with polyclonal anti-NR2B as described (Nateri *et al*, 2004). For microarray and RT-PCR analysis, total mRNA was isolated from dissected hippocampus, using RNeasy Mini-kit according to the manufacturer's instructions (Qiagen). Microarray analysis was performed at the CR-UK core service facility using 18 U133 Plus 2.0 arrays (Affymetrix). For RT-PCRs, cDNA was synthesized using Invitrogen Superscript reagents according to the manufacturer's instructions. RT-PCR was performed using a Chromo4 Fluorescence machine (MJ Research), and the data were analysed using the Opticon Monitor3 software. The reaction mixture consisted of 2.5 μ l of cDNA, 12.5 μ l of 2 \times SyberGreen

PCR master mix (Applied Bioscience), 2 μ l of 5 μ M forward and 2 μ l of 5 μ M reverse primer in a 25 μ l reaction volume.

The following primer sequences were used:

F-NR1, 5'-GAGGGCCGGCAGCGCAGAAGCGCCTG-3'; R-NR1, 5'-GTAGATGCCCACTTGACCACAGGA-3'; F-NR2A, 5'-GCACTATGATCATGGCTGACAAGG-3'; R-NR2A, 5'-GTCTCCGGCTTCTGTCTGCTCCG-3'; F-NR2B, 5'-GACCGGAAGATCCAGGGGGTGGTG-3'; R-NR2B, 5'-GTAGATCCTTCTCGTGGGTGTGTAG-3'; F-EphrinB1, 5'-GTGC GGCCAGAGCAGGCGGCTGCTT-3'; R-EphrinB1, 5'-GGACGATGTAG ACAGGTGCCCCGTAG-3'; F-EphrinB2, 5'-GGCTGGTACTATACCCAC AGATAGGAG-3'; R-EphrinB2, 5'-GTCTGCAGTCCTTACTGGTATGAT AACG-3'; F-EphrinB3, 5'-TCTCCTAGTTATGAGTCTAC-3'; R-EphrinB3, 5'-CGCAGGGCTATTCCTAGTCC-3'; F-CEBP, 5'-GGCGAGCAGCAGC GCGCCATCG-3'; R-CEBP, 5'-GGACGACGACGACTGGACAGGCTG-3'.

IHC staining

Brain samples were fixed overnight in 10% neutral buffered formalin, transferred into 70% ethanol and embedded in paraffin block. Sections (4 μ m were cut from each block and placed on glass-charged slides. Slides were subjected to a standard dewaxing protocol as follows: 2 \times 10 min in xylene, 2 min sequentially in 100, 95, 90, 80, 70, 50, 25% ethanol and 5 min in PBS. For P-ERK staining, after antigen retrieval (12 min of microwave in 0.1 M sodium citrate pH = 6), slides were blocked for 1 h, the P-ERK antibody (Cell Signalling; 1 mg/ml) was used at the final dilution 1:250 in combination with a mouse on mouse kit (Dako ARK) and was developed according to the manufacturer's instructions. IHC stainings for neuronal markers were performed as described (Raivich *et al*, 2004).

Supplementary data

Supplementary data are available at *The EMBO Journal* Online (<http://www.embojournal.org>).

Acknowledgements

We thank JJ Haigh and E Janda for providing reagents. We are grateful to L Collinson, S Gschmeissner, I Rosewell and B Spencer-Dene for technical help. We thank I Mansuy, E Sahai, G Schiavo and J Villadiego for critical reading of the manuscript. C Gebhardt is funded by a Rahel-Hirsch fellowship (Charité). O Kann is supported by the Deutsche Forschungsgemeinschaft (SFB-507, SFB-665). The London Research Institute is funded by Cancer Research UK.

References

- Behrens A, Sibia M, Wagner EF (1999) Amino-terminal phosphorylation of c-Jun regulates stress-induced apoptosis and cellular proliferation. *Nat Genet* **21**: 326–329
- Binder DK, Routbort MJ, McNamara JO (1999) Immunohistochemical evidence of seizure-induced activation of trk receptors in the mossy fiber pathway of adult rat hippocampus. *J Neurosci* **19**: 4616–4626
- Chang L, Karin M (2001) Mammalian MAP kinase signalling cascades. *Nature* **410**: 37–40
- Chen Z, Gibson TB, Robinson F, Silvestro L, Pearson G, Xu B, Wright A, Vanderbilt C, Cobb MH (2001) MAP kinases. *Chem Rev* **101**: 2449–2476
- Chenard BL, Menniti FS (1999) Antagonists selective for NMDA receptors containing the NR2B subunit. *Curr Pharm Des* **5**: 381–404
- Contractor A, Rogers C, Maron C, Henkemeyer M, Swanson GT, Heinemann SF (2002) Trans-synaptic Eph receptor-ephrin signalling in hippocampal mossy fiber LTP. *Science* **296**: 1864–1869
- Cull-Candy S, Brickley S, Farrant M (2001) NMDA receptor subunits: diversity, development and disease. *Curr Opin Neurobiol* **11**: 327–335
- Fan G, Beard C, Chen RZ, Csankovszki G, Sun Y, Siniatia M, Biniszkiwicz D, Bates B, Lee PP, Kuhn R, Trumpp A, Poon C, Wilson CB, Jaenisch R (2001) DNA hypomethylation perturbs the function and survival of CNS neurons in postnatal animals. *J Neurosci* **21**: 788–797
- Fischer AM, Katayama CD, Pages G, Pouyssegur J, Hedrick SM (2005) The role of erk1 and erk2 in multiple stages of T cell development. *Immunity* **23**: 431–443
- Gebhardt C, Cull-Candy SG (2006) Influence of agonist concentration on AMPA and kainate channels in CA1 pyramidal cells in rat hippocampal slices. *J Physiol* **573**: 371–394
- Gonzales RA, Brown LM, Jones TW, Trent RD, Westbrook SL, Leslie SW (1991) N-methyl-D-aspartate mediated responses decrease with age in Fischer 344 rat brain. *Neurobiol Aging* **12**: 219–225
- Grunwald IC, Korte M, Adelmann G, Plueck A, Kullander K, Adams RH, Frotscher M, Bonhoeffer T, Klein R (2004) Hippocampal plasticity requires postsynaptic ephrinBs. *Nat Neurosci* **7**: 33–40
- He XP, Kotloski R, Nef S, Luikart BW, Parada LF, McNamara JO (2004) Conditional deletion of TrkB but not BDNF prevents epileptogenesis in the kindling model. *Neuron* **43**: 31–42
- He XP, Minichiello L, Klein R, McNamara JO (2002) Immunohistochemical evidence of seizure-induced activation of trkB receptors in the mossy fiber pathway of adult mouse hippocampus. *J Neurosci* **22**: 7502–7508
- Heinemann U, Gabriel S, Schuchmann S, Eder C (1999) Contribution of astrocytes to seizure activity. *Adv Neurol* **79**: 583–590
- Henderson JT, Georgiou J, Jia Z, Robertson J, Elowe S, Roder JC, Pawson T (2001) The receptor tyrosine kinase EphB2 regulates NMDA-dependent synaptic function. *Neuron* **32**: 1041–1056
- Herbert TP, Tee AR, Proud CG (2002) The extracellular signal-regulated kinase pathway regulates the phosphorylation of 4E-BP1 at multiple sites. *J Biol Chem* **277**: 11591–11596
- Kann O, Kovacs R, Njunting M, Behrens CJ, Otahal J, Lehmann TN, Gabriel S, Heinemann U (2005) Metabolic dysfunction during neuronal activation in the *ex vivo* hippocampus from chronic epileptic rats and humans. *Brain* **128**: 2396–2407

- Kelleher III RJ, Govindarajan A, Jung HY, Kang H, Tonegawa S (2004) Translational control by MAPK signaling in long-term synaptic plasticity and memory. *Cell* **116**: 467–479
- Kew JN, Kemp JA (1998) An allosteric interaction between the NMDA receptor polyamine and ifenprodil sites in rat cultured cortical neurones. *J Physiol* **512** (Part 1): 17–28
- Kim KS, Lee MK, Carroll J, Joh TH (1993) Both the basal and inducible transcription of the tyrosine hydroxylase gene are dependent upon a cAMP response element. *J Biol Chem* **268**: 15689–15695
- Klein R (2004) Eph/ephrin signaling in morphogenesis, neural development and plasticity. *Curr Opin Cell Biol* **16**: 580–589
- Logroscino G, Hesdorffer DC, Cascino G, Hauser WA, Coeytaux A, Galobardes B, Morabia A, Jallon P (2005) Mortality after a first episode of status epilepticus in the United States and Europe. *Epilepsia* **46** (Suppl 11): 46–48
- Lonze BE, Ginty DD (2002) Function and regulation of CREB family transcription factors in the nervous system. *Neuron* **35**: 605–623
- Mazzucchelli C, Vantaggiato C, Ciamei A, Fasano S, Pakhotin P, Krezel W, Welzl H, Wolfer DP, Pages G, Valverde O, Marowsky A, Porrazzo A, Orban PC, Maldonado R, Ehrenguber MU, Cestari V, Lipp HP, Chapman PF, Pouyssegur J, Brambilla R (2002) Knockout of ERK1 MAP kinase enhances synaptic plasticity in the striatum and facilitates striatal-mediated learning and memory. *Neuron* **34**: 807–820
- McHugh TJ, Jones MW, Quinn JJ, Balthasar N, Coppari R, Elmquist JK, Lowell BB, Fanselow MS, Wilson MA, Tonegawa S (2007) Dentate gyrus NMDA receptors mediate rapid pattern separation in the hippocampal network. *Science* **317**: 94–99
- Merlo D, Cifelli P, Cicconi S, Tancredi V, Avoli M (2004) 4-Aminopyridine-induced epileptogenesis depends on activation of mitogen-activated protein kinase ERK. *J Neurochem* **89**: 654–659
- Minichiello L, Korte M, Wolfer D, Kuhn R, Unsicker K, Cestari V, Rossi-Arnaud C, Lipp HP, Bonhoeffer T, Klein R (1999) Essential role for TrkB receptors in hippocampus-mediated learning. *Neuron* **24**: 401–414
- Mody I, Heinemann U (1987) NMDA receptors of dentate gyrus granule cells participate in synaptic transmission following kindling. *Nature* **326**: 701–704
- Murai KK, Pasquale EB (2004) Eph receptors, ephrins, and synaptic function. *Neuroscientist* **10**: 304–314
- Nakazawa T, Komai S, Tezuka T, Hisatsune C, Umemori H, Semba K, Mishina M, Manabe T, Yamamoto T (2001) Characterization of Fyn-mediated tyrosine phosphorylation sites on GluR epsilon 2 (NR2B) subunit of the N-methyl-D-aspartate receptor. *J Biol Chem* **276**: 693–699
- Nateri AS, Riera-Sans L, Da Costa C, Behrens A (2004) The ubiquitin ligase SCFFbw7 antagonizes apoptotic JNK signaling. *Science* **303**: 1374–1378
- Niehof M, Manns MP, Trautwein C (1997) CREB controls LAP/C/EBP beta transcription. *Mol Cell Biol* **17**: 3600–3613
- Otani N, Nawashiro H, Yano A, Katoh H, Ohnuki A, Miyazawa T, Shima K (2003) Characteristic phosphorylation of the extracellular signal-regulated kinase pathway after kainate-induced seizures in the rat hippocampus. *Acta Neurochir Suppl* **86**: 571–573
- Palmer GC (2001) Neuroprotection by NMDA receptor antagonists in a variety of neuropathologies. *Curr Drug Targets* **2**: 241–271
- Pearson G, Robinson F, Beers Gibson T, Xu BE, Karandikar M, Berman K, Cobb MH (2001) Mitogen-activated protein (MAP) kinase pathways: regulation and physiological functions. *Endocr Rev* **22**: 153–183
- Prybylowski K, Wenthold RJ (2004) N-Methyl-D-aspartate receptors: subunit assembly and trafficking to the synapse. *J Biol Chem* **279**: 9673–9676
- Raivich G, Bohatschek M, Da Costa C, Iwata O, Galiano M, Hristova M, Nateri AS, Makwana M, Riera-Sans L, Wolfer DP, Lipp HP, Aguzzi A, Wagner EF, Behrens A (2004) The AP-1 transcription factor c-Jun is required for efficient axonal regeneration. *Neuron* **43**: 57–67
- Ranganathan A, Yazicioglu MN, Cobb MH (2006) The nuclear localization of ERK2 occurs by mechanisms both independent of and dependent on energy. *J Biol Chem* **281**: 15645–15652
- Robinson MJ, Stippes SA, Goldsmith E, White MA, Cobb MH (1998) A constitutively active and nuclear form of the MAP kinase ERK2 is sufficient for neurite outgrowth and cell transformation. *Curr Biol* **8**: 1141–1150
- Sananbenesi F, Fischer A, Schrick C, Spiess J, Radulovic J (2002) Phosphorylation of hippocampal Erk-1/2, Elk-1, and p90-Rsk-1 during contextual fear conditioning: interactions between Erk-1/2 and Elk-1. *Mol Cell Neurosci* **21**: 463–476
- Sebolt-Leopold JS, Herrera R (2004) Targeting the mitogen-activated protein kinase cascade to treat cancer. *Nat Rev Cancer* **4**: 937–947
- Sweatt JD (2004) Mitogen-activated protein kinases in synaptic plasticity and memory. *Curr Opin Neurobiol* **14**: 311–317
- Takasu MA, Dalva MB, Zigmond RE, Greenberg ME (2002) Modulation of NMDA receptor-dependent calcium influx and gene expression through EphB receptors. *Science* **295**: 491–495
- Tamaru M, Yoneda Y, Ogita K, Shimizu J, Nagata Y (1991) Age-related decreases of the N-methyl-D-aspartate receptor complex in the rat cerebral cortex and hippocampus. *Brain Res* **542**: 83–90
- Thomas GM, Huganir RL (2004) MAPK cascade signalling and synaptic plasticity. *Nat Rev Neurosci* **5**: 173–183
- Treisman R (1996) Regulation of transcription by MAP kinase cascades. *Curr Opin Cell Biol* **8**: 205–215
- Tronche F, Kellendonk C, Kretz O, Gass P, Anlag K, Orban PC, Bock R, Klein R, Schutz G (1999) Disruption of the glucocorticoid receptor gene in the nervous system results in reduced anxiety. *Nat Genet* **23**: 99–103
- Ueda T, Watanabe-Fukunaga R, Fukuyama H, Nagata S, Fukunaga R (2004) Mnk2 and Mnk1 are essential for constitutive and inducible phosphorylation of eukaryotic initiation factor 4E but not for cell growth or development. *Mol Cell Biol* **24**: 6539–6549
- Weeber EJ, Sweatt JD (2002) Molecular neurobiology of human cognition. *Neuron* **33**: 845–848
- Wenk GL, Walker LC, Price DL, Cork LC (1991) Loss of NMDA, but not GABA-A, binding in the brains of aged rats and monkeys. *Neurobiol Aging* **12**: 93–98
- Wood MW, VanDongen HM, VanDongen AM (1996) The 5'-untranslated region of the N-methyl-D-aspartate receptor NR2A subunit controls efficiency of translation. *J Biol Chem* **271**: 8115–8120
- Zhang X, Odom DT, Koo SH, Konkright MD, Canettieri G, Best J, Chen H, Jenner R, Herbolsheimer E, Jacobsen E, Kadam S, Ecker JR, Emerson B, Hogenesch JB, Unterman T, Young RA, Montminy M (2005) Genome-wide analysis of cAMP-response element binding protein occupancy, phosphorylation, and target gene activation in human tissues. *Proc Natl Acad Sci USA* **102**: 4459–4464